**Hanna R, Crowther J, Bulsara P, Wang X, Moore D, Birch-Machin MA.**
**Optimised detection of mitochondrial DNA strand breaks.**
***Mitochondrion* 2018,**

# Optimised detection of mitochondrial DNA strand breaks

Rebecca Hanna[1], Jonathan M. Crowther[2], Pallav A. Bulsara[3], Xuying Wang[4], David J. Moore[3], and Mark A. Birch-Machin[1]

[1] Dermatological Sciences, Medical School, Newcastle University, Newcastle, NE2 4HH, UK
[2] GSK Consumer Healthcare, 980 Great West Road, Brentford, Middlesex, TW8 9GS, UK
[3] GSK Consumer Healthcare, 184 Liberty Corner Rd, Warren, NJ, 07059, USA
[4] GSK Consumer Healthcare, 1250 S. Collegeville Road, Collegeville, PA, 19426-0989, USA

## Corresponding Author:

Professor Mark A Birch-Machin
Dermatological Sciences
Institute of Cellular Medicine
The Medical School
Newcastle University
Framlington Place
Newcastle Upon Tyne
NE2 4HH
United Kingdom
Tel: +44 (0) 191 208 5841
Email: mark.birch-machin@ncl.ac.uk

## Abstract

Intrinsic and extrinsic factors that induce cellular oxidative stress damage tissue integrity and promote ageing, resulting in accumulative strand breaks to the mitochondrial DNA (mtDNA) genome. Limited repair mechanisms and close proximity to superoxide generation make mtDNA a prominent biomarker of oxidative damage. Using human DNA we describe an optimised long-range qPCR methodology that sensitively detects mtDNA strand breaks relative to a suite of short mitochondrial and nuclear DNA housekeeping amplicons, which control for any variation in mtDNA copy number. An application is demonstrated by detecting 30-fold mtDNA damage in human skin cells induced by hydrogen peroxide and solar simulated radiation.

## Keywords

Mitochondrial DNA damage; biomarker; oxidative stress; long range qPCR; human; skin

# 1. Introduction

Mitochondrial DNA (mtDNA) content, lesions, methylation, deletions and mutations are widespread biomarkers of disease and ageing (Wallace, 2010; Tulah and Birch-Machin, 2013). This is particularly true of highly metabolic or proliferative tissues, such as the nervous, muscular and endocrine systems (Hudson *et al.*, 2016). Oxidative stress is thought to be a major contributor of the mtDNA damage and this tends to induce random strand breaks. The mtDNA genome is located in close proximity to the site of reactive oxygen species (ROS) production and multiple copies exist within each cell. These factors make mtDNA particularly vulnerable to the effects of oxidative stress, exacerbated further by the fact that mtDNA has limited repair mechanisms and lacks protective histones (Anderson *et al.*, 2014). Indeed, the mutation frequency of mtDNA is approximately 50-fold higher than nuclear DNA (Berneburg *et al.*, 2000). As the integrity of mtDNA is essential for mitochondrial function, the accumulation of mutations can result in dysfunctional mitochondrial subunits (Anderson *et al.*, 2014). The dysfunctional mitochondria are thought to contribute to increased ROS production, leading to further oxidative damage to mitochondria in a continuous cycle (Birch-Machin and Bowman, 2016).

Various quantitative polymerase chain reaction (qPCR) assays have been used to detect relative amounts of DNA damage between samples (Hunter *et al.*, 2010). Primers specific to the mitochondrial genome (mtDNA) allow for experimental use of total DNA, without mitochondrial isolation. This additionally permits cross-examination of both genomes in the same DNA sample (Santos *et al.*, 2006). We and others have previously described assay methodologies that detects strand breaks in mtDNA which work on the premise that lesions or significant mutation will significantly halt DNA polymerase progression (Ray *et al.*, 2000; Passos *et al.*, 2007). Although some lesions are an exception to this premise, oxidative stress does not induce uniform damage (Wallace, 2002; Sikorsky *et al.*, 2007) and so a long range PCR methodology is employed. The methods used transition from long range PCR to qPCR though incorporation of fluorescent dyes, whereby a more damaged sample will require a greater number of cycles to produce the same amount of amplicon product (Santos *et al.*, 2006). The length of the amplicon increases the region screened for damage, and therefore heightens assay sensitivity.

Here we amplify an 11kb region of the 16.5kb human mitochondrial genome spanning 11 of the 13 genes encoding functional components of the electron transport chain (ETC) and a majority of the D-loop region which initiates mtDNA replication and transcription (Li *et al.*, 2012). This method has substantially improved on previously published versions of the 11kb long PCR assay by not only significantly scaling down the amount of starting DNA (ng) and the assay reaction volume, but also ensuring the validation of generated results by controlling for any variation in copy number. This is attained by the simultaneous amplification of a unique combination of two small mtDNA specific amplicons from different regions of the genome, relative to one from the single copy nuclear β2M gene. This has several key benefits, firstly widening the scope of clinical samples that can now be comparatively screened for mtDNA damage and secondly ensuring equal mtDNA content within the context of total DNA samples.

The resulting assay method described in this study represents a reproducible screening tool for a wide-ranging biomarker, with the added advantage of a simple data analysis approach. The primers in this method can be experimentally used with the DNA of any human tissue. An application of this methodology is demonstrated in detection of mtDNA damage following the separate treatment of human primary skin cells by hydrogen peroxide and solar simulated radiation.

# 2. Methods

## 2.1 Cell Culture and DNA Damage

Patient skin cells were isolated from adult male samples of the Freeman Hospital, Newcastle upon Tyne. All human tissue work adhered to the guidelines outlined by the Newcastle and North Tyneside Research Ethics Committee (Ref 08/H0906/95+5), and Newcastle upon Tyne Hospitals NHS Foundation Trust. Primary Keratinocytes were used experimentally from passages 1 to 3 and maintained in Epi-Life supplemented with 1% human keratinocyte growth supplement (HKGS; Thermo Scientific) and 1% Streptomycin-Penicillin-Amphotericin B (PSA; Lonza). Primary Fibroblasts were used experimentally from passages 1 to 6 and maintained in high glucose DMEM (4.5g/L glucose and L-glutamine; Lonza), supplemented with 10% foetal bovine serum (FBS; Lonza) and 1% PSA.

DNA damage was induced with 150µM Hydrogen Peroxide ($H_2O_2$; Sigma) or full spectrum solar radiation. All $H_2O_2$ dosing was performed in non-supplemented cell-specific medium, incubated for 1 or 2 hours at room temperature, and light protected with aluminium foil. Solar irradiation (SR) was performed with a Newport Solar Simulator (Model 91282-1000) at a dose of 2.16 standard erythemal dose (SED) (Diffey, 1991). Cells were grown in 3.2cm$^2$ dishes and irradiated in phenol-red free non-supplemented DMEM with lids removed. Non-irradiated controls were foil wrapped throughout irradiation. Each damage stimulus was performed in three keratinocyte and three fibroblasts donors.

## 2.2 DNA isolation and Quantification

Total DNA was extracted with a QiaAMP DNA mini kit (Qiagen) and quantified by NanoDrop spectrophotometer (Thermo Scientific). Isolated DNA was of high quality ($A_{260}/A_{280} > 1.8$) and stored at -20$^o$C.

## 2.3 Oligonucleotides

Primer sequences for all qPCR assays are as outlined in Table 1, alongside their respective published source. Sequence specificity was additionally verified using Sanger Institute Artemis, PrimerBLAST, and UCSC genome browsers. 'Optimised Application Oligos' for qPCR were synthesized by Eurofins Genomics, and reconstituted to 100µM in IDTE buffer (10mM Tris, pH 8, 0.1mM EDTA). Single use aliquots of ~~11kb~~ working primers (10µM) were prepared

in IDTE buffer and stored at -20°C. ~~Working primers for housekeeping assays were diluted in PCR-grade water and stored at -20°C.~~

| Primer Set | | Base Sequence (5' to 3') | Nucleotide Numbers | $T_M$ ($\pm 1^oC$) | Primer Efficiency (%) | Source |
|---|---|---|---|---|---|---|
| **11,095bp (*mtDNA*)** | DLB (*forward*); OLA (*reverse*) | ATGATGTCTGTGTGGAAA GTGGCTGTGC<br><br>GGGAGAAGCCCCGGCAG GTTTGAAGC | chrM: 282 + 5756 | 84 | 93.5* | Kleinle *et al.* (1997) |
| **83bp *(mtDNA)*** | IS1 *(forward)* IS2 *(reverse)* | GATTTGGGTACCACCCAA GTATTG<br><br>AATATTCATGGTGGCTGGC AGTA | chrM: 16042 + 16124 | 80 | 93.5 | Koch *et al.* (2001) |
| **87bp *(mtDNA)*** | DS1 F *(forward)* DS1 R *(reverse)* | ACTACAACCCTTCGCTGA CG<br><br>GCGGTGATGTAGAGGGT GAT | chrM: 3442 + 3528 | 82 | 92 | Rothfuss *et al.* (2010) |
| **93bp *(nuclear DNA β2M gene)*** | hB2M F2 *(forward)* hB2M R2 *(reverse)* | GCTGGGTAGCTCTAAACA ATGTATTCA<br><br>CCATGTACTAACAAATGT CTAAAATGGT | chr15: 39523 + 39617 | 79 | 102 | Malik *et al.* (2011) |

**Table 1: Primer Pair Sequences for qPCR. Product melt temperature, primer efficiency (%) and source are included. *Primer efficiency of 93.5% only within the dynamic linear range (see Figure 2).**

## 2.4 Amplification of 11kb mtDNA amplicons using qPCR

Amplicons spanning 11kb of the 16.5kb mitochondrial DNA genome (Figure 1(A)) were amplified using a SYBR Green qPCR assay. This 11kb region spans 11 of the 13 genes encoding functional components of the electron transport chain (ETC) and a majority of the D-loop region which initiates mtDNA replication and transcription (Li *et al.*, 2012). SYBR Green I binds to double stranded mtDNA and fluoresces relative to a passive ROX reference dye. Fluorescence (ΔRn) increases exponentially to amount of amplicon, and is measured at the end of each cycle. As illustrated in Figure 1(B) data is analysed according the comparative $C_t$ method ($\Delta\Delta C_t$) whereby a more damaged sample will require more cycles to produce the same amount of amplicon product (Santos *et al.*, 2006). The method was performed on a 96 well StepOnePlus™ machine (Applied Biosystems), with mastermix composition and settings outlined in Tables 2 and 3. The Expand Long Range PCR System (Sigma) was used alongside SYBR Green I DNA dye (10,000X in DMSO; Lonza) and ROX passive reference dye (Applied

Biosystems). To achieve 5X SYBR Green working concentration, a 1µl frozen aliquot was diluted in 2ml IDTE buffer. Each sample was assayed in triplicate with a standard deviation threshold of ≤ 0.4 $C_t$. $C_t$ threshold was manually adjusted to the linear range on StepOnePlus™ v2.3 software, and melt curve analysis used to determine product size.

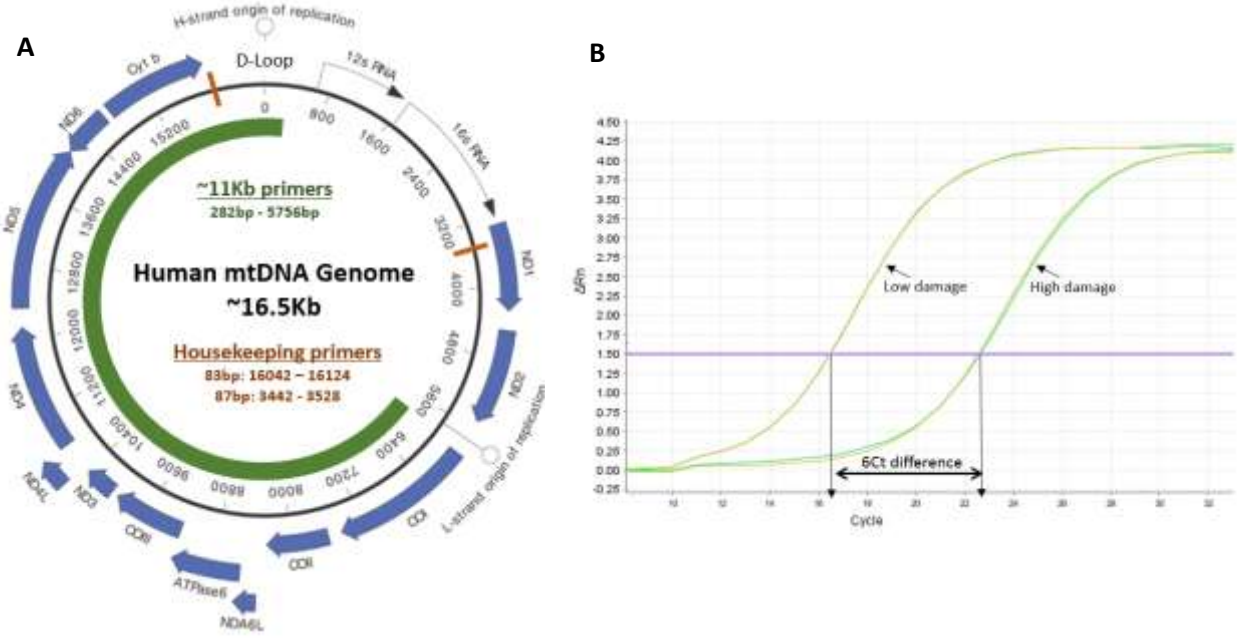


**Figure 1: (A) Schematic representation of the ~11kb region (green) amplified from each ~16.5kb human mitochondrial DNA (mtDNA) genome. It is a circular molecule with an inner light (L) strand and outer heavy (H) strand. The 11kb region amplified contains 11 of 13 genes (blue arrows) encoding polypeptide components of the mitochondrial electron transport chain. It also covers a large portion of the non-coding D-loop control region. Small housekeeping regions are indicated in orange. (B) Amplification plot indicating $C_t$ difference between a highly damaged and low damaged sample. Fluorescent threshold (1.5ΔRn) has been set within the linear range of exponential amplification.**

| Mastermix Composition | Volume (µl) | Final Concentration |
|---|---|---|
| PCR grade $H_20$ | 12.7 | N/A |
| Expand Long Template Buffer 2, with 27.5 mM $MgCl_2$ (10X concentrated) | 2.0 | 1X Buffer (2.75mM $MgCl_2$) |
| PCR nucleotide mix (10mM dATP, dCTP, dGTP, and dTT) | 1.0 | 500 µM |
| D1B primer (10µM; diluent: 10mM Tris, pH8, 0.1mM EDTA (IDTE)) | 0.6 | 0.3µM (300µM Tris, 0.3µM EDTA) |
| OLA primer (10µM; diluent: IDTE) | 0.6 | 0.3 µM (300µM Tris, 0.3µM EDTA) |
| SYBR Green I (5X concentrated; diluent: IDTE) | 0.4 | 0.1X Sybr Green I (300µM Tris, 0.3µM EDTA) |
| ROX passive reference dye (50X concentrated) | 0.4 | 1X |
| Expand Long Template Enzyme Mix (5U/µl) | 0.3 | 0.075U |
| Mastermix Total | 18.0 | |
| DNA (6ng/µl) | 2.0 | |
| Reaction Total | 20.0 | |

**Table 2: Reagents for 11kb qPCR assay.**

| Stage | Temperature | Time (minutes) | Cycles |
|---|---|---|---|
| Initial Denaturation | 94.0 | 2.00 | 1 |
| Denaturation | 94.0 | 0.15 | 10 *(Acquire at end of step)* |
| Annealing | 60.0 | 0.30 | |
| Extension | 72.0 | 9.00 | |
| Denaturation | 94.0 | 0.15 | 25 *(Acquire at end of step)* |
| Annealing | 60.0 | 0.30 | |
| Extension | 68.0 | 8.50 (+10 seconds per cycle) | |
| StepOnePlus Melt Curve Stage | | | |

**Table 3: Amplification settings for 11kb qPCR assay**

## 2.5 Validation of 11kb mtDNA amplicons

During initial optimisation, amplified qPCR products were additionally analysed on a Gel-Red (Biotium) stained 0.8% w/v agarose gel, and visualised using a Li-Cor Odyssey Fc system. Positive 11kb bands were cross-referenced with StepOnePlus melt curve analysis whereby each amplicon reached peak maximum at the same temperature. To establish the dynamic linear range and therefore optimal starting amount of DNA (ng), standard curves were simultaneously performed on one qPCR plate using untreated HDFn cell line, primary fibroblast and primary keratinocyte DNA. Each sample was serially diluted (1:2) from

100ng/µl to 3.125ng/µl. To identify the precise linear range, several smaller ranging standard curves were then performed (e.g. 20ng/µl to 5ng/µl). Linear regression analysis was used to calculate primer efficiency whereby E = $2^{(-1/slope)}$. Percentage efficiency (%) was calculated by (E-1) x 100.

## 2.6 Quality Control: Amplification of Housekeeping Amplicons

Small regions of mtDNA-specific (83bp or 87bp) and a single copy nuclear DNA β2M gene (93bp) were simultaneously amplified using a SYBR Green based qPCR assay (Sigma). The method was performed on a 96 well StepOnePlus™ machine (Applied Biosystems), with mastermix composition and settings outlined in Tables 4 and 5. Each sample was assayed in triplicate with a standard deviation threshold of ≤ 0.4 $C_t$. $C_t$ threshold was manually adjusted to the linear range on StepOnePlus™ v2.3 software, and melt curve analysis used to determine product size. The standard curve for each primer pair were simultaneously performed on one qPCR plate using untreated primary fibroblast DNA. Each sample was serially diluted (1:2) from 100ng/µl to 1.56ng/µl. Linear regression analysis was performed as for 11kb standard curve.

| Mastermix Composition | Volume (µl) | Final Concentration |
|---|---|---|
| PCR grade $H_20$ | 8.25 | N/A |
| Forward primer (10µM) | 1 | 0.4 µM |
| Reverse primer (10µM) | 1 | 0.4 µM |
| SYBR® Green JumpStart™ Taq ReadyMix™ (2X) | 12.5 | 1X |
| ROX passive reference dye (100X) | 0.25 | 1X |
| Mastermix Total | 23.0 | |
| DNA | 2.0 | |
| Reaction Total | 25.0 | |

**Table 4: Reagents for 83bp/87bp/93bp housekeeping qPCR**

| Stage | Temperature | Time (minutes) | Cycles |
|---|---|---|---|
| Initial Denaturation | 94.0 | 2.00 | 1 |
| Denaturation | 94.0 | 0.15 | 35 |
| Annealing | 60.0 | 0.45 | *(Acquire at end of step)* |
| Extension | 72.0 | 0.45 | |
| Final Extension | 72.0 | 2.00 | |
| StepOnePlus Melt Curve Stage | | | |

**Table 5: Amplification settings for 83bp/87bp/93bp housekeeping qPCR**

# 3. Results

## 3.1 Validation of the 11kb qPCR strand break assay

### 3.1.1 Identification of a dynamic linear DNA range

A series of mean standard curves evaluated the dynamic linear range and primer efficiency across a range of 6.25ng-200ng starting total DNA (Figure 2). A series of smaller standard curves (data not shown) narrowed the linear range too approximately 10-50ng, with 12ng selected as an optimal and economical starting DNA amount. Extending the regression analysis outside this range progressively reduced calculated primer efficiency (%) as low as 62%. However within this range (as indicated by dashed box), linear regression analysis determined a correlation coefficient ($R^2$) of 0.91, and primer efficiency (%) of 93.5%. There was no difference seen between DNA extracted from different cell types, as demonstrated by the negligible error bars of Figure 2).

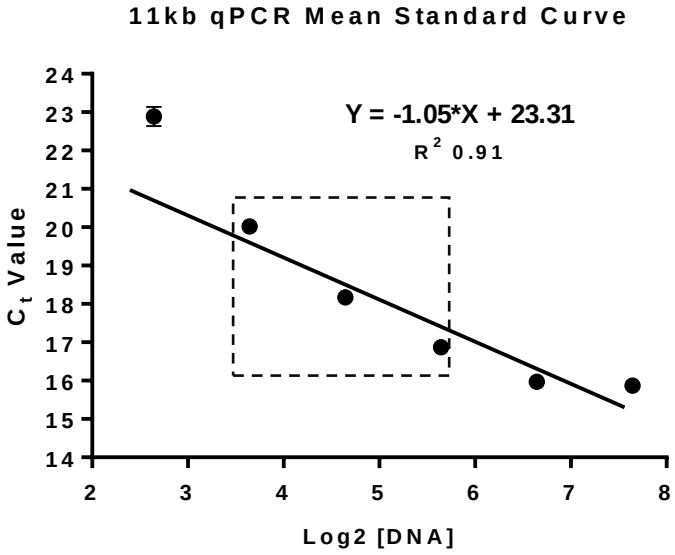


| DNA (ng) | Log2 [DNA] |
|---|---|
| 200 | 7.64 |
| 100 | 6.64 |
| 50 | 5.64 |
| 25 | 4.64 |
| 12.5 | 3.64 |
| 6.25 | 2.64 |

**Figure 2: Mean standard curve for 11kb qPCR determined the linear range to lie between 10-50ng, whereby a doubling of DNA concentration corresponded to a 1 CT difference. Mean + SEM data of primary keratinocyte, primary fibroblast and HDFn cell line DNA (n=9, per data point).**

### 3.1.2 Clarification of the 11kb product amplification

Positive 11kb bands were determined by StepOnePlus melt curve analysis whereby each amplicon reached peak maximum at the same temperature of 84$^{o}$C ± 1 (Figure 3). Agarose gel analysis of all standard curve products (6-200ng) demonstrated 11kb bands. For samples ≤50ng positive bands correlated to the correct size, with absence of non-specific binding or primer- dimers (Figure 3). However for 50-200ng the 11kb bands were accompanied by smears of unamplified DNA and bi-peak melt curves (data not shown).

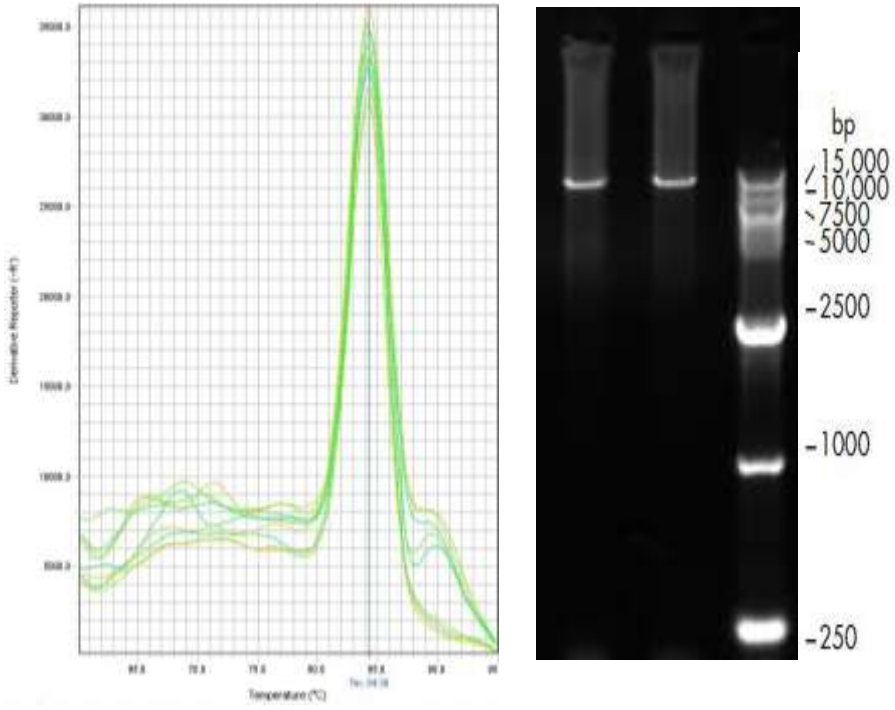


**Figure 3: Melt curve analysis and agarose gel show positive 11kb amplicons, with no evidence of non-specific binding or primer-dimer.**

### 3.1.3 Determining equal amounts of starting mtDNA between samples and in relation to a nuclear DNA housekeeping gene.

To establish equal starting amounts of mtDNA between samples, small regions of mtDNA specific (83bp or 87bp) and a single copy nuclear DNA β2M gene (93bp) were simultaneously amplified. The relative amount of mtDNA in treated versus untreated samples, was additionally normalised to the amount of β2M (93bp; gDNA) within those samples.

A comparative $C_t$ method was used to determine the fold difference, whereby $2^{\Delta\Delta Ct}$ = 2^ ((Ct, mtDNA, untreated – $C_t$, gDNA, untreated)) - (($C_t$, mtDNA, treated - $C_t$, gDNA, treated). All compared samples were between 1$C_t$ (± 0.3) of each other. This is demonstrated in Figure 4 (D) showing equal amounts of starting mtDNA and nuclear DNA in both solar irradiated and non-irradiated primary skin cells. If an experimental treatment increases or reduces the

amount of intact mtDNA within the sample, the fold difference determines the ratio adjustment required between total DNA samples.

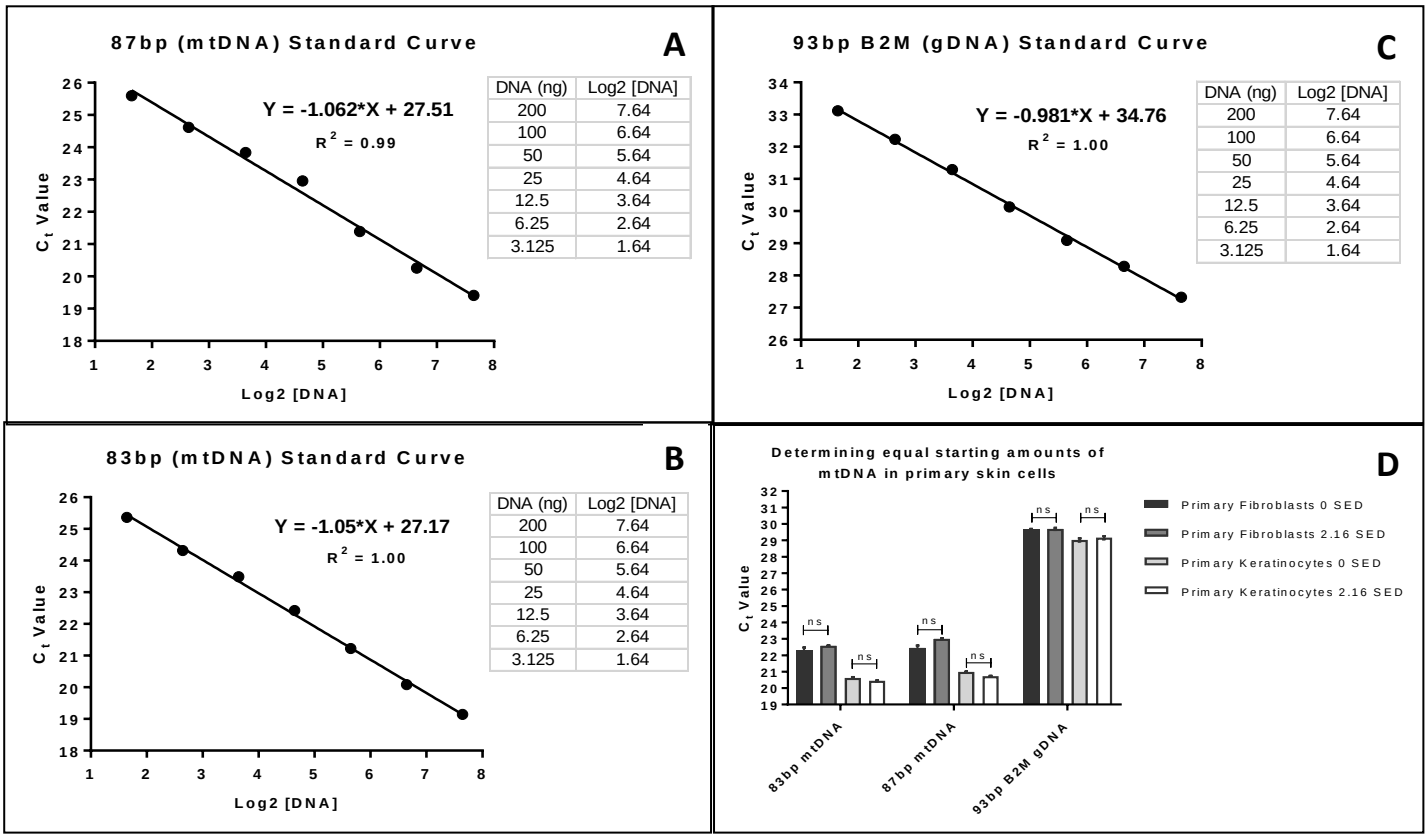


**Figure 4: (A-C) Standard curves (mean + SEM) of the 83bp, 87bp and 93bp qPCR housekeeping assays, were the dynamic linear range of each spanned 3-200ng. (D) Bar chart showing equal amounts of starting mtDNA in both solar irradiated and non-irradiated primary skin cells.**

## 3.2 Sensitive detection of mtDNA strand breaks in $H_2O_2$/SR treated human primary skin cells

Treatment of both human skin derived keratinocytes and fibroblasts by either hydrogen peroxide ($H_2O_2$) or solar simulated radiation (SR) induced mtDNA strand breaks at significantly detectable levels, as determined by the modified 11kb qPCR assay. Relative to untreated cells there is approximately 18–38 fold ($2^{4.3}$–$2^{6.2}$) greater damage and this was not due to unequal amounts of starting mtDNA. The simultaneous housekeeping mtDNA and nuclear DNA PCR assays not only confirmed equal loading of mtDNA in the assay, but that the treatment did not alter mtDNA content in relation to the nuclear gene. It is of interest that a similar degree of damage is induced in both skin types by both the hydrogen peroxide and solar simulated light.

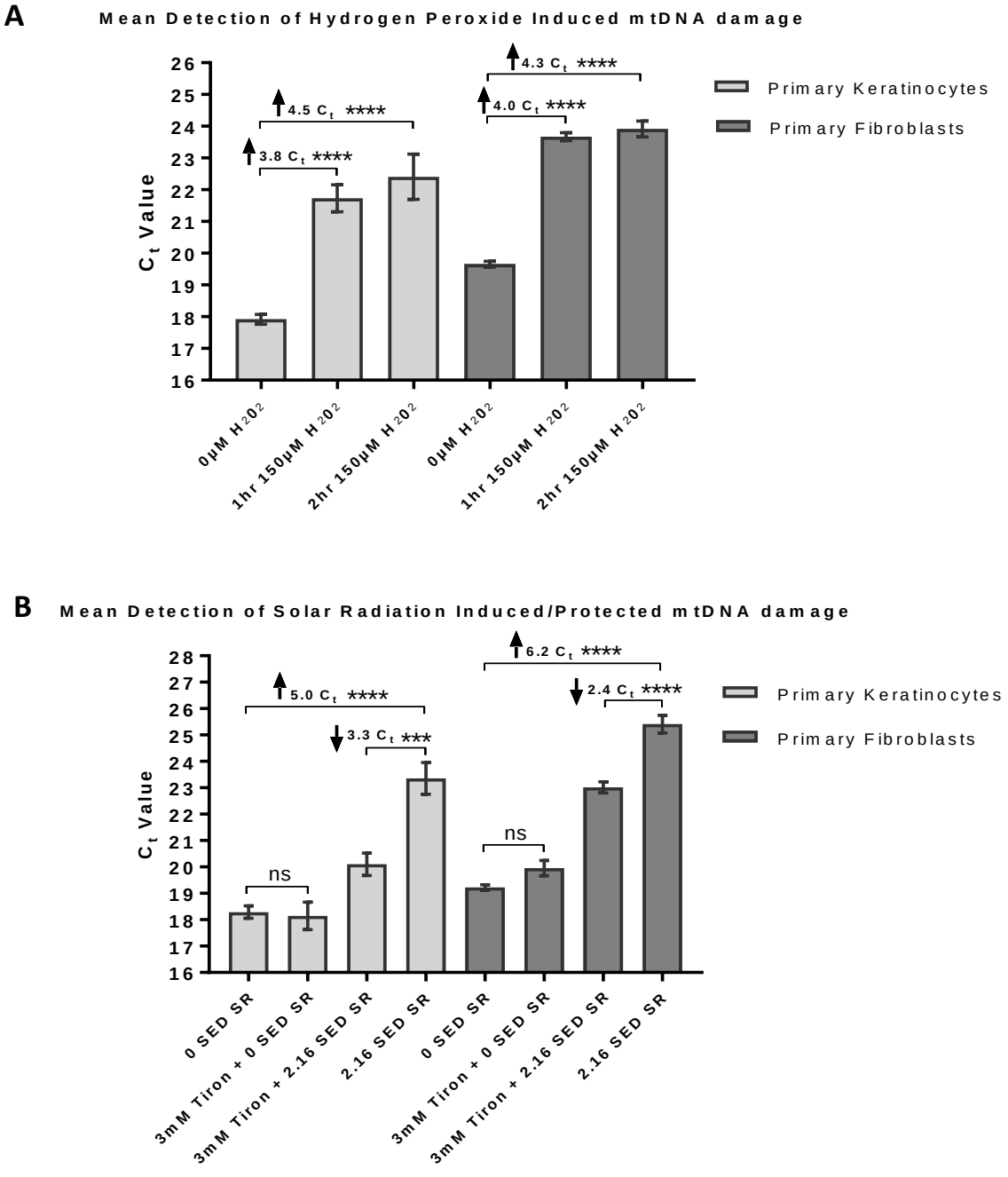


**Figure 5: <u>Detection of $H_2O_2$ (A) or SR (B) induced mtDNA damage in human primary skin cells. Results generated from three primary adult Keratinocyte or Fibroblast donors (N), treated with 150μM $H_2O_2$ (A) or 2.16 SED (standard erythema dose) complete SR (B).</u> A dose of 2.16 SED is estimated to be the equivalent of 2 hrs in the Mediterranean sun at noon during the summer months as an SED is 100 Joules per square meter. <u>In addition, detection of mtDNA protection is demonstrated through pre-incubation with a mitochondria-permeable compound (Tiron (PBS vehicle); Graph B)</u>. Each sample was performed in triplicate (n), whereby SEM bars represent donor variability. Statistical difference determined by One-Way Anova with Tukey's Post-Hoc Analysis. **** p <0.0001, <u>*** p = 0.0001, ns p>0.05</u>; N=3, n=9 per cell type**

## 4. Discussion

This method has improved on previously published versions of the 11kb assay arising from our research group (Ray *et al.*, 2000; Passos *et al.*, 2007). Firstly we report a substantial 76% reduction in the amount of starting DNA (from 50ng (per well) to 12ng) and 60% reduction in reaction volume (from 50µl to 20µl). This has been verified by the appropriate dilution curves and melt curve analysis (Figures 2 and 3). This has an obvious benefit for those applications where the clinical samples are small and DNA amount is limiting for multiple analysis, or where large screening is required and the economy of small sample volumes permits the analysis. Standard curves were used to determine the qPCR efficiency for each primer pair, whereby 100% equates to a doubling of amplicon product per cycle (Taylor *et al.*, 2010). The dilutions where this occurs lie within the linear dynamic range, and determines the optimal amount of starting template (ng) to use. Whilst a 10-fold dilution series is generally favoured, we have used a 2-fold approach because the linear range for large amplicons is small. For this approximate 11kb amplicon, the region of high efficiency (93.5%) spans only 10-50ng and reduces considerably outside this range. The 11kb standard curve data was indistinguishable when performed on DNA from different cell types (primary or cell line). Although primers were reconstituted and diluted in IDTE buffer, the final EDTA concentration supported oligo integrity without diminishing amplification. A direct comparison with PCR grade water was found to disrupt primer integrity over time, resulting in dimerization with melt temperatures of 79-80$^{o}$C. However with IDTE buffer consistent 11kb products occur without artefact, observed as a single melt temperature peak of 84$^{o}$C.

The second key improvement has centred on the unique combination of the simultaneous amplification of two small mtDNA specific amplicons from different regions of the mitochondrial genome as well as one from the single copy nuclear β2M gene to ensure equal mtDNA content within the context of total DNA samples. We have therefore expanded our housekeeping methodology to incorporate the simultaneous amplification of an 83bp and/or 87bp amplicon from different regions of the mtDNA genome and a 93bp amplicon of a single copy nuclear β2M gene. The use of these regions and their amplification conditions have been verified by the appropriate dilution curves (Figure 4). The comparable $C_t$ values obtained from both mtDNA specific regions (Fig. 4(D)) provides reassurance that the regions are not damaged or co-amplifying from the nuclear genome (Malik *et al.*, 2011). Detecting mtDNA relative to nuclear DNA eliminates dilution bias, and validates $C_t$ changes detected by the 11kb assay. A comparative $C_t$ analysis ($2^{\Delta\Delta Ct}$) determines the fold difference between mtDNA and nuclear DNA levels of untreated and treated samples. To avoid dilution error, the same diluted sample is typically used for sequential runs of housekeeping and 11kb assays.

The primers in this method can be experimentally used with the DNA of any human tissue. An application of this methodology is demonstrated in detection of mtDNA damage following the separate treatment of human primary skin cells by hydrogen peroxide and solar simulated radiation. Assay sensitivity is demonstrated through an 18–38 fold increase in detection of induced mtDNA strand breaks relative to untreated fibroblasts and keratinocytes. Tiron was

selected to demonstrate localised mtDNA protection as it is mitochondrial membrane permeable, a potent chelator and free radical scavenger (Yong *et al.*, 2012). Tiron pre-incubation correlated with a significantly reduced $C_t$ value, demonstrating localised protection against solar radiation induced mtDNA damage. Whilst the use of solar irradiation is an environmental stressor specific to skin, excess $H_2O_2$ is a hallmark of oxidative stress in an abundance of internal tissues (Halliwell *et al.*, 2000) and further confirms the application of this modified and optimised assay to many cell types subjected particularly to oxidative stress.

## 5. Conflict of Interests

The authors have no competing interests to declare.

## 6. Funding Sources

This work was supported by the Biotechnology and Biological Sciences Research Council (BBSRC CASE award with GlaxoSmithKline; Grant number BH151766). GlaxoSmithKline were involved in the decision to submit the article for publication and in reviewing the report.

## 7. Manuscript Printing

Figures 1 and 3 should be printed in colour.

## 8. References

Anderson, A., Bowman, A., Boulton, S.J., Manning, P. and Birch-Machin, M.A. (2014) 'A role for human mitochondrial complex II in the production of reactive oxygen species in human skin', *Redox Biology*, 2, pp. 1016-1022.

Berneburg, M., Plettenberg, H. and Krutmann, J. (2000) 'Photoaging of human skin', *Photodermatology, Photoimmunology & Photomedicine*, 16(6), pp. 239-244.

Birch-Machin, M.A. and Bowman, A. (2016) 'Oxidative stress and ageing', *British Journal of Dermatology*, 175, pp. 26-29.

Diffey, B.L. (1991) 'Solar ultraviolet radiation effects on biological systems', *Physics in Medicine and Biology*, 36(3), p. 299.

Halliwell, B., Clement, M.V. and Long, L.H. (2000) 'Hydrogen peroxide in the human body', *FEBS Letters*, 486(1), pp. 10-13.

Hudson, L., Bowman, A., Rashdan, E. and Birch-Machin, M.A. (2016) 'Mitochondrial damage and ageing using skin as a model organ', *Maturitas*, 93, pp. 34-40.

Hunter, S.E., Jung, D., Di Giulio, R.T. and Meyer, J.N. (2010) 'The QPCR assay for analysis of mitochondrial DNA damage, repair, and relative copy number', *Methods*, 51(4), pp. 444-451.

Kleinle, S., Wiesmann, U., Superti-Furga, A., Krähenbühl, S., Boltshauser, E., Reichen, J. and Liechti-Gallati, S. (1997) 'Detection and characterization of mitochondrial DNA rearrangements in Pearson and Kearns-Sayre syndromes by long PCR', *Human Genetics*, 100(5), pp. 643-650.

Koch, H., Wittern, K.-P. and Bergemann, J. (2001) 'In Human Keratinocytes the Common Deletion Reflects Donor Variabilities Rather Than Chronologic Aging and can be Induced by Ultraviolet A Irradiation', *Journal of Investigative Dermatology*, 117(4), pp. 892-897.
Li, H., Liu, D., Lu, J. and Bai, Y. (2012) 'Physiology and Pathophysiology of Mitochondrial DNA', in Scatena, R., Bottoni, P. and Giardina, B. (eds.) *Advances in Mitochondrial Medicine*. Dordrecht: Springer Netherlands, pp. 39-51.
Malik, A.N., Shahni, R., Rodriguez-de-Ledesma, A., Laftah, A. and Cunningham, P. (2011) 'Mitochondrial DNA as a non-invasive biomarker: Accurate quantification using real time quantitative PCR without co-amplification of pseudogenes and dilution bias', *Biochemical and Biophysical Research Communications*, 412(1), pp. 1-7.
Passos, J.F., Saretzki, G., Ahmed, S., Nelson, G., Richter, T., Peters, H., Wappler, I., Birket, M.J., Harold, G., Schaeuble, K., Birch-Machin, M.A., Kirkwood, T.B.L. and von Zglinicki, T. (2007) 'Mitochondrial Dysfunction Accounts for the Stochastic Heterogeneity in Telomere-Dependent Senescence', *PLoS Biology*, 5(5), p. e110.
Ray, A.J., Turner, R., Nikaido, O., Rees, J.L. and Birch-Machin, M.A. (2000) 'The Spectrum of Mitochondrial DNA Deletions is a Ubiquitous Marker of Ultraviolet Radiation Exposure in Human Skin', *Journal of Investigative Dermatology*, 115(4), pp. 674-679.
Rothfuss, O., Gasser, T. and Patenge, N. (2010) 'Analysis of differential DNA damage in the mitochondrial genome employing a semi-long run real-time PCR approach', *Nucleic Acids Research*, 38(4), pp. e24-e24.
Santos, J.H., Meyer, J.N., Mandavilli, B.S. and Van Houten, B. (2006) 'Quantitative PCR-Based Measurement of Nuclear and Mitochondrial DNA Damage and Repair in Mammalian Cells', in Henderson, D.S. (ed.) *DNA Repair Protocols: Mammalian Systems*. Totowa, NJ: Humana Press, pp. 183-199.
Sikorsky, J.A., Primerano, D.A., Fenger, T.W. and Denvir, J. (2007) 'DNA damage reduces Taq DNA polymerase fidelity and PCR amplification efficiency', *Biochemical and Biophysical Research Communications*, 355(2), pp. 431-437.
Taylor, S., Wakem, M., Dijkman, G., Alsarraj, M. and Nguyen, M. (2010) 'A practical approach to RT-qPCR—Publishing data that conform to the MIQE guidelines', *Methods*, 50(4), pp. S1-S5.
Tulah, A.S. and Birch-Machin, M.A. (2013) 'Stressed out mitochondria: The role of mitochondria in ageing and cancer focussing on strategies and opportunities in human skin', *Mitochondrion*, 13(5), pp. 444-453.
Wallace, D.C. (2010) 'Mitochondrial DNA mutations in disease and aging', *Environmental and Molecular Mutagenesis*, 51(5), pp. 440-450.
Wallace, S.S. (2002) 'Biological consequences of free radical-damaged DNA bases1,2 1Guest Editor: Miral Dizdaroglu 2This article is part of a series of reviews on "Oxidative DNA Damage and Repair." The full list of papers may be found on the homepage of the journal', *Free Radical Biology and Medicine*, 33(1), pp. 1-14.
Yong, F., Xiao-Hui, H., Zhi-Gang, J., Mang-Hua, X., Zhu-Ying, G. and Feng-Hou, G. (2012) 'Tiron protects against UVB-induced senescence-like characteristics in human dermal fibroblasts by the inhibition of superoxide anion production and glutathione depletion', *Australasian Journal of Dermatology*, 53(3), pp. 172-180.